Journal of Mathematical Sciences and Modelling, 7(1) (2024) 33-44
Research Article

Journal of Mathematical Sciences and Modelling

Journal Homepage: www.dergipark.gov.tr/jmsm
ISSN 2636-8692
DOI: http://dx.doi.org/10.33187/jmsm.1417160

Improving Tuberculosis Diagnosis using Explainable Artificial Intelligence in Medical Imaging

Cem Özkurt[1,2]

[1]*Department of Computer Engineering, Faculty of Technology,Sakarya University of Applied Science, Sakarya, Turkey*
[2]*AI and Data Science Research and Application Center, Sakarya University of Applied Science, Sakarya, Turkey*

Article Info

Keywords: *Artificial Intelligence, Deep Learning, Explainable AI, Medical Imaging, Tuberculosis Diagnosis*
2010 AMS: *68T07, 68T10*
Received: *9 January 2024*
Accepted: *1 March 2024*
Available online: *9 March 2024*

Abstract

The integration of artificial intelligence (AI) applications in the healthcare sector is ushering in a significant transformation, particularly in developing more effective strategies for early diagnosis and treatment of contagious diseases like tuberculosis. Tuberculosis, a global public health challenge, demands swift interventions to prevent its spread. While deep learning and image processing techniques show potential in extracting meaningful insights from complex radiological images, their accuracy is often scrutinized due to a lack of explainability.

This research navigates the intersection of AI and tuberculosis diagnosis by focusing on explainable artificial intelligence (XAI). A meticulously designed deep learning model for tuberculosis detection is introduced alongside an exploration of XAI to unravel complex decisions.

The core belief is that XAI, by elucidating diagnostic decision rationale, enhances the reliability of AI in clinical settings. Emphasizing the pivotal role of XAI in tuberculosis diagnosis, this study aims to impact future research and practical implementations, fostering the adoption of AI-driven disease diagnosis methodologies for global health improvement.

1. Introduction

In today's healthcare landscape, the integration of artificial intelligence (AI) applications is heralding a significant transformation. This transformation is particularly focused on developing more effective strategies for the early diagnosis and treatment of contagious diseases, such as tuberculosis. Tuberculosis, as a global public health challenge, requires rapid diagnosis and effective treatment to prevent its spread. In this context, the potent capabilities of deep learning and image processing techniques to extract meaningful insights from complex radiological images come to the forefront. However, the accuracy of these sophisticated models and their roles in disease diagnosis processes are frequently scrutinized due to a lack of explainability.

This research endeavors to navigate the intersection of AI and tuberculosis diagnosis by delving into the realm of explainable artificial intelligence (XAI). The study is grounded in the premise that elucidating the decision-making processes of AI models is imperative, especially in critical domains like healthcare. Our exploration unfolds with the introduction of a meticulously designed deep learning model tailored for tuberculosis detection. Concurrently, in this study an investigative journey into the realm of XAI is embarked upon, with methods being sought to unravel the intricate decisions formulated by the model.

The crux of our inquiry lies in the conviction that XAI, by shedding light on the rationale behind diagnostic decisions, holds the potential to augment the dependability and acceptance of AI applications in clinical settings. By accentuating the pivotal role of explainable artificial intelligence in the context of tuberculosis diagnosis, this study aspires to cast a meaningful ripple effect on forthcoming research endeavors and practical implementations in the field. The broader embrace of AI-driven methodologies for disease diagnosis holds promise in advancing global initiatives aimed at curtailing the impact of tuberculosis through the optimization of early intervention and treatment protocols.

Email address and ORCID number: cemozkurt@subu.edu.tr, 0000-0002-1251-7715
Cite as "Cem Özkurt, *Improving Tuberculosis Diagnosis using Explainable Artificial Intelligence in Medical Imaging*, J. Math. Sci. Model., 7(1) (2024), 33-44"

2. Related Works

The TX-CNN method is a proposed approach for detecting tuberculosis in chest X-ray images [1]. In this method, convolutional neural networks are trained to learn and detect the characteristic features of TB in chest X-ray images. It is believed that TX-CNN has the potential to surpass existing methods in TB screening and diagnosis.

Pre-trained CNNs are convolutional neural networks trained on large datasets beforehand and successful in general object recognition tasks. In this study, pre-trained CNNs have been utilized as feature extractors for TB detection, and competitive results have been achieved when used for this purpose [2]. Pre-trained models can be trained with less labeled data and can yield successful results on more general datasets as well. Due to these characteristics, they require fewer computational resources and can be applied more quickly compared to models trained from scratch, especially for specific tasks such as TB detection.

The potential of XAI within the industry has been thoroughly examined, particularly focusing on the implementation of natural language processing solutions at companies like Trivago, shedding light on the challenges faced by commercial AI solutions in this field [3].

Research on the use of chest X-ray images for tuberculosis diagnosis and localization has been reviewed [4]. In these studies, the value and effectiveness of chest X-rays as a primary screening tool for tuberculosis diagnosis have been addressed. Additionally, emphasis has been placed on how chest X-ray images can be utilized to determine the localization of TB lesions and monitor the progression of the disease.

It demonstrates the significant role that Convolutional Neural Networks (CNNs) can play in the accurate and automatic detection and classification of TB. The use of pre-trained CNNs highlights the potential applications for early and accurate diagnosis of TB [5]. This approach may enable healthcare professionals and medical systems to identify and manage TB cases more effectively, leading to faster treatment of patients and preventing the spread of the disease.

They have presented an innovative methodology for the temporal and spatial characterization of toxic substances known as BTEX. Utilizing receptor-oriented air circulation modeling and AI techniques, they have demonstrated the possibility of extracting valuable information from a single measurement point [6].

A method for predicting the impact of climate change on building cooling energy consumption using XAI has been developed. Through scenario-based approaches, meaningful and reliable projections have been provided to decision-makers, aiming to achieve climate-resilient and sustainable development goals [7].

The application of XAI in deep learning-based medical image analysis has been extensively explored. Emphasizing the importance of transparency, particularly in high-risk areas such as medical image analysis, their overview highlights the increasing demand in this field [8].

The use of machine learning techniques as a tool for tuberculosis (TB) diagnosis represents a significant advancement in the healthcare sector [9]. It suggests that machine learning algorithms could be utilized to provide additional assistance to healthcare professionals in TB diagnosis, thereby improving the treatment process by enabling faster and more accurate recognition of TB.

Automated machine learning models have also been successful in predicting TB [10]. Machine learning models trained on synthetic data have shown the ability to predict TB with high accuracy and sensitivity. This could play a crucial role in the early detection and treatment of the disease.

TB-Net is a proposed deep learning model for screening high-risk populations and early detection of TB using chest X-ray imaging [11]. This customized deep learning model could be integrated into widespread screening programs for TB and play a significant role in community-based healthcare services. TB-Net is considered to be a critical tool in ensuring early diagnosis and initiating treatment.

They have examined a new dataset using deep learning algorithms and visualized outputs with Grad-CAM, demonstrating the application of XAI in diagnosing paratuberculosis from histopathological images [12].

Three different XAI methods have been evaluated on CNN models designed for classifying lung cancer from histopathological images. These studies are considered a significant step towards transparency in black-box models [13].

A clinician-assisted intelligent workflow for retinal imaging has been proposed. This approach aims to enhance transparency in decisions related to systemic disease detection, thereby increasing reliability in clinical practice [14].

Tuberculosis detection in chest X-rays is an important method for recognizing the disease [15]. Machine learning and deep learning methods have been systematically addressed in this area. This study may facilitate the development of new and improved algorithms for accurately identifying TB in chest X-rays.

Efforts have been made to develop multi-scale Local Interpretable Model-Agnostic Explanations (LIME) for image classification. This work demonstrates the ability of XAI methods applied to CNN models to provide explanations through heatmaps at coarse to finer scales [16].

The utility of current neuroscience knowledge in designing biologically hierarchical and modular architecture (BHMA) models of the brain has been the focus. This perspective offers insights into the use of these models in spatial learning tasks [17].

Modern deep learning methods and XAI approaches have been employed to address skin cancer detection. These studies are evaluated as a significant step in improving diagnosis in medical image analysis and laying the groundwork for future developments [18].

3. Materials and Methods

3.1. Dataset

A collaborative team of researchers from Qatar University in Doha, Qatar, and Dhaka University in Bangladesh, in partnership with collaborators from Malaysia and medical experts from Hamad Medical Corporation and Bangladesh, has created a comprehensive chest X-ray database. This database encompasses a collection of images, including Tuberculosis (TB) positive cases as well as Normal images. In our latest release, 700 TB images are publicly available, while an additional 2800 TB images can be accessed through a straightforward negotiation process via the NIAID TB portal [19]. Additionally, the database contains 3500 images representing normal cases. Image samples from the dataset are provided, as seen in Figure 3.1.

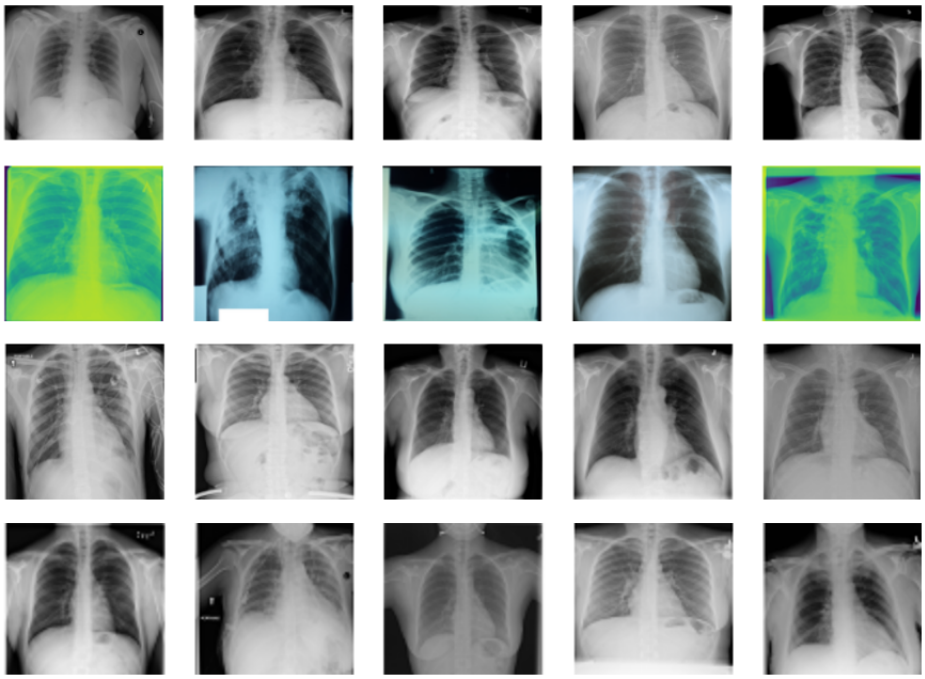

Figure 3.1: Tuberculosis (TB) Chest X-ray Database dataset examples

3.2. Convolutional Neural Network (CNN)

Convolutional Neural Networks (CNNs) play a critical role, especially in medical imaging applications. Despite their effectiveness in learning complex patterns from image data, understanding the internal decision-making processes of these networks is challenging [20]. Therefore, the internal decision-making processes of these networks are referred to as a ”black box” and criticized. For example, an illustration of a ”black box” example of this Convolutional Neural Network model is seen in Figure 3.2.
In the model used in our research, there are three Convolutional Layers (Conv2D). The sizes of these layers are 32, 64, and 128 respectively. These layers are used to extract feature maps of size (3x3) from input images of size (150x150) and to learn these features hierarchically. Following each convolutional layer, there is a MaxPooling Layer (MaxPooling2D). Max pooling is applied to reduce the size of feature maps and focus on important features. Subsequently, Fully Connected Layers (Dense) come into play. The Flatten layer flattens the feature maps extracted by the convolutional layers, making these features suitable for the utilization of fully connected layers. The location of these layers is referred to as a ”black box.” The output layer of the model includes a sigmoid activation function for the binary classification task, allowing the model to express the result as a probability between 0 and 1. For a better understanding of the model used in this study, it is modeled as seen in Figure 3.3.

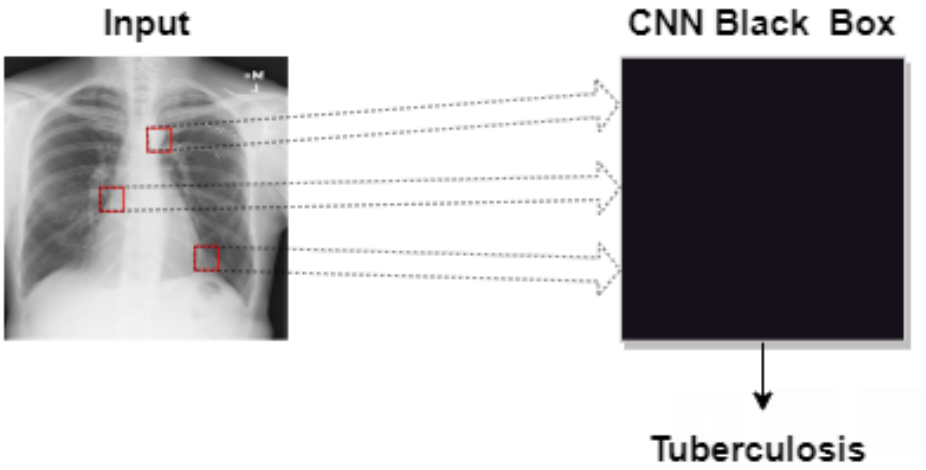

Figure 3.2: Example of the ”black box” model of Convolutional Neural Network

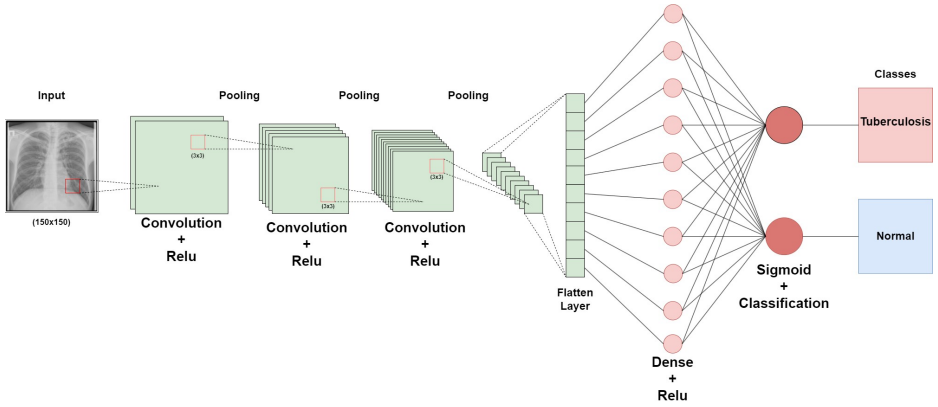

Figure 3.3: Used convolutional neural network (CNN) model

3.3. Explainable Artificial Intelligence (XAI)

Explainable Artificial Intelligence (XAI) is an effort aimed at elucidating the internal workings of complex artificial intelligence models, often referred to as black boxes. Understanding these models can be challenging due to their intricate structures and millions of parameters [21]. XAI has been developed to overcome this challenge and make the decisions of these models transparent and understandable for humans. Transparency contributes significantly to reliability and broader acceptance, particularly in industries like healthcare. The example illustrated in Figure 3.4 visually depicts the impact of Explainable Artificial Intelligence on a black box model.
While advanced deep learning models, particularly in fields like medical imaging, can be effective, uncertainties about how these models make decisions may undermine their reliability. XAI techniques, such as SHAP and LIME, are employed to reduce these uncertainties and elucidate the internal decision processes of black box models. In this context, techniques like SHAP and LIME provide effective tools to understand which features a model focuses on when making a specific prediction or diagnosis.

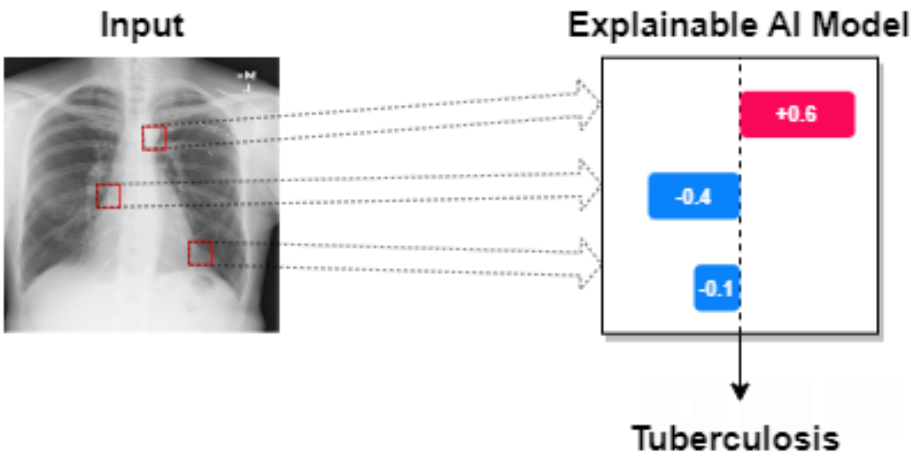

Figure 3.4: The impact of explainable AI on the black box

3.4. SHAP (SHapley Additive exPlanations)

Explainable Artificial Intelligence (XAI), particularly when using SHAP (SHapley Additive exPlanations), allows us to discern the contribution of each feature in chest X-ray data to the model's predictions. For example, in the case of Tuberculosis diagnosis, SHAP can explain pixel by pixel which features in X-ray images make the most significant contribution, either negatively or positively, to the model's decision [22]. Transparency in this decision-making process reinforces confidence in the capabilities of the artificial intelligence model.

$$\phi_i = \sum_{S \subseteq N\{i\}} \frac{|S|!(M-|S|-1)!}{M!}[f_x(S \cup i) - f_x(S)] \tag{3.1}$$

As seen in Equation 3.1, Shapley values are a method that fairly assesses the impact of a feature on the model output in the presence of other features. $\Delta\omega_i$ represents the Shapley value for feature i, and to compute this value, the sum of the contributions of the feature's impact on the model output across coalitions is calculated. The set S represents the total number of variables affecting the model output, and N denotes the number of levels of variables influencing the model output. M specifies the number of variable selections for a particular feature. The calculation is performed over the entire set S, excluding the i feature, with the condition $S \subseteq N \setminus \{i\}$. The contribution of each coalition is weighted based on the size of the S set, and the result relies on the difference between the union of the variables influencing the model output $(S \cup \{i\})$ and the previous state with the S set. These contributions are then summed with appropriate weights to obtain the Shapley value for feature i. These computations are used to fairly measure the contribution of a feature to the model prediction.

$$f_x(S) = E[f(x)|x_s] \tag{3.2}$$

As seen in Equation 3.2, f_x represents the change in the output included by Shapley values for a specific feature. x_S represents the set of observed conditions in the event of the occurrence, and $\mathbb{E}$ symbolizes the expectation operator. The formula is used to calculate the expected value of the model output under a specific feature set, expressing the concept of conditional expectation in probability theory.

$$g(z^{'}) = \phi_0 + \sum_{i=1}^{M} \phi_i Z_i^{'} = bias + \sum featureContribution \tag{3.3}$$

In Equation 3.3, $g(z')$ represents the output of a prediction, which is computed as the sum of a constant term ϕ_0 (usually representing a bias value) and the contributions of each input feature Z_i', typically expressed as weights ϕ_i, multiplied and summed. This formulation is used to understand to what extent each input feature contributes to a prediction. The SHAP method utilizes Shapley values to determine these contributions, elucidating the net effect of an input feature on the prediction. This is a useful tool for understanding how predictions are generated by a model and determining which features are important, particularly in the analysis of complex models and large datasets.

Let's take an example from the Tuberculosis (TB) Chest X-ray Database to better understand how SHAP works. When applied to this example, SHAP generates explanations as seen in Figure 3.5 and Figure 3.6.

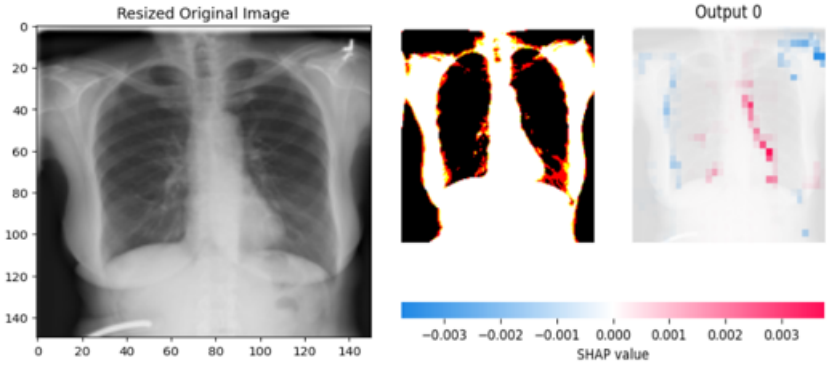

Figure 3.5: SHAP interpretation of the first randomly selected image from the dataset.

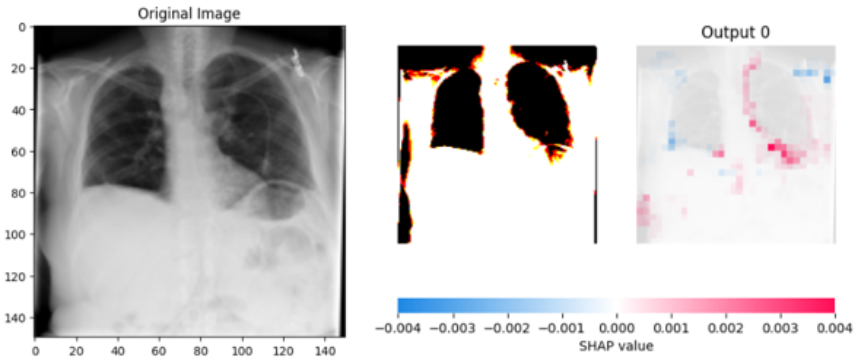

Figure 3.6: SHAP interpretation of the second randomly selected image from the dataset.

3.5. LIME (Local Interpretable Model-agnostic Explanations)

Local Interpretable Model-agnostic Explanations (LIME) is a technique specifically designed in the field of Explainable Artificial Intelligence (XAI) to make the decisions of complex artificial intelligence models, commonly referred to as "black boxes," more understandable. This method is adapted to locally explain the prediction decision of a model for a specific data point or instance.

$$\xi(x) = \underset{g \in G}{\operatorname{argmax}}\, \Im(f, g, \pi_x) + \Omega(g) \tag{3.4}$$

As seen in Equation 3.4, when g is selected, it chooses the best explanation model within the set G using the arg max operator. The selected model is determined by the part $I(f, g, \pi_x)$ that measures how well g mimics f in the π_x region of g. The $I(f, g, \pi_x)$ function measures how successfully G imitates f in the region defined by π_x, and demonstrates the interpretability of the model's behavior around a specific input example. Additionally, the $\Omega(g)$ function measures the complexity of the selected explanation model and determines how simple or complex the explanation is.

To better understand how LIME works, the differences between the images taken from the Tuberculosis (TB) Chest X-ray Database and used in Figures 3.5 and 3.6 are highlighted by applying LIME. The generated explanations by LIME are depicted in Figures 3.7 and 3.8.

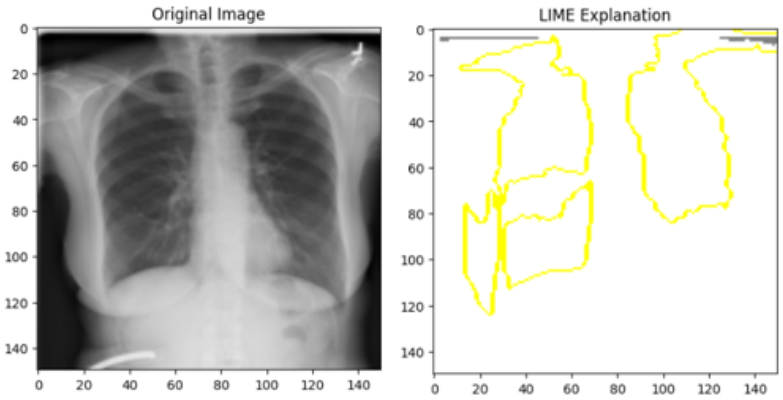

Figure 3.7: LIME output of the image taken in figure 3.5.

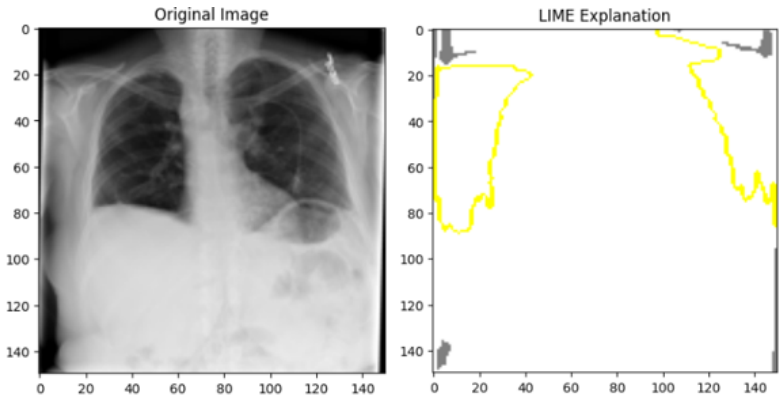

Figure 3.8: LIME output of the image taken in figure 3.6

3.6. Experimental study and results

In this study, the classified Tuberculosis (TB) Chest X-ray Database using a Convolutional Neural Network (CNN) model is used. The interpretability of the classification model is enhanced by integrating two explainable artificial intelligence techniques, namely SHAP and LIME. By comparing the results, it was observed that SHAP could better explain the classification of X-ray images related to Tuberculosis (TB) compared to LIME.
The training of the proposed convolutional neural network model and the interpretability of explainable artificial intelligence models were conducted. This process took place on a computer with the hardware specifications as seen in Table (3.1).

Class	**Image Number**
Memory (RAM)	16GB (2x8GB) DDR4 2933MHz
Processor	Intel i7-10750H-2,60GHz Turbo Boost 5,0GHz
Graphics Card, Memory	Nvidia GTX1650 Ti 4GB GDDR6

Table 3.1: Hardware specifications of the computer used in the paper.

A confusion matrix is used to evaluate the performance of a classification model. This matrix is created by comparing the predictions of a classification model on a set of test data for which the true values are known. It allows for a clear analysis of the model's successes, errors, and mispredictions. The confusion matrix of the model, along with the values TP (True Positive) 3494, TN (True Negative) 692, FP (False Positive) 6, FN (False Negative) 8, is presented in Figure 3.9. These values provide detailed insights into the reliability and accuracy of the classification model.

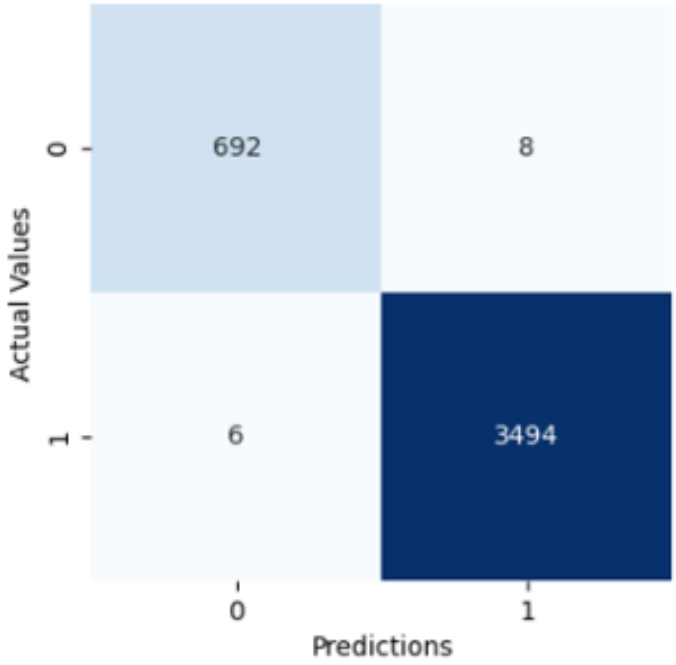

Figure 3.9: Convolutional neural networks confusion matrix outputs.

TP (True Positive): Instances where the model correctly predicts the positive class.
TN (True Negative): Instances where the model correctly predicts the negative class.
FP (False Positive): Instances where the model incorrectly predicts the positive class.
FN (False Negative): Instances where the model incorrectly predicts the negative class.
Performance metrics such as precision, recall, and accuracy are obtained from the confusion matrix values. Precision measures how many of the samples predicted as positive are actually positive. It expresses the ratio of true positives to the total positive predictions, as shown in Formula 3.5.

$$\text{Precision} = \frac{TP}{TP+FP} \tag{3.5}$$

Recall measures how many of the true positives are detected. It expresses the ratio of true positives to the total number of positive examples, as shown in Formula 3.6.

$$\text{Recall} = \frac{TP}{TP+FN} \tag{3.6}$$

Accuracy expresses the ratio of correctly predicted examples to the total number of examples. It is a metric that evaluates the overall model performance, as shown in Formula 3.7.

$$\text{Accuracy} = \frac{TP+TN}{TP+TN+FP+FN} \tag{3.7}$$

F1-score balances precision and recall. This metric tends to minimize both false positives and false negatives, especially in balanced classification problems. Formula 3.8 illustrates the F1-score.

$$F1 = 2 \times \frac{\text{Precision} \times \text{Recall}}{\text{Precision} + \text{Recall}} \tag{3.8}$$

The evaluation metrics for the Convolutional Neural Network (CNN) model used in the study, including F1 score, precision, recall, and support, are provided in Table 3.2.

	precision	recall	f1-score	support
NORMAL	0.91	0.87	0.89	234
TUBERCULOSIS	0.93	0.95	0.94	390

Table 3.2: Classification report

An example of artificial intelligence explainable to the TP example of the confusion matrix:

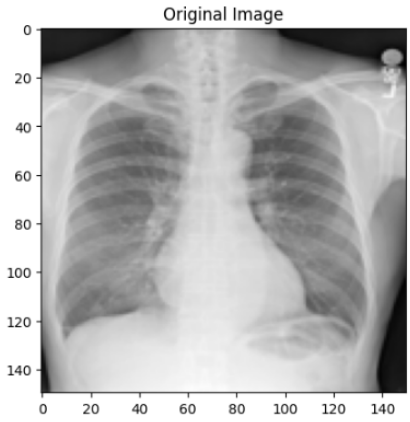

Figure 3.10: Original image

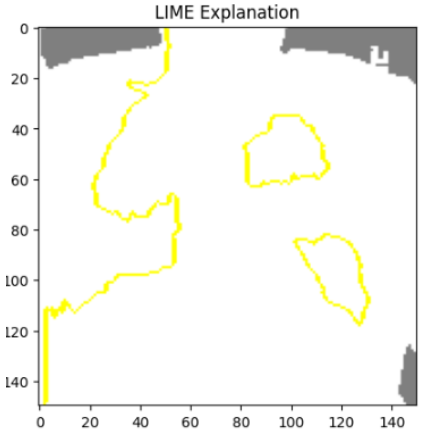

Figure 3.11: LIME output

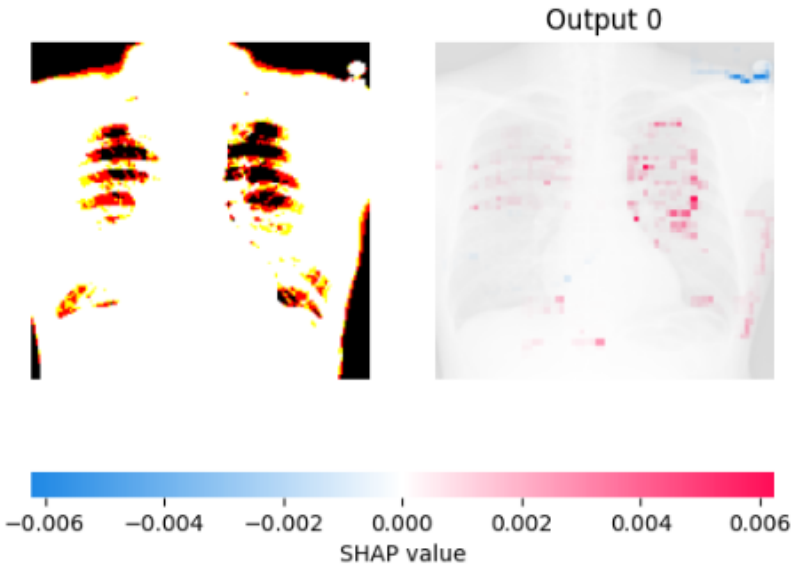

Figure 3.12: SHAP output

The confusion matrix derived from the results of our CNN model applied to the Tuberculosis (TB) Chest X-ray Database is specifically illustrated with a randomly selected example of Tuberculosis-free (TP) instances in Figure 3.10. The results obtained by applying two

interpretable artificial intelligence models, SHAP and LIME, to this example are presented in Figures 3.11 and 3.12, respectively. As observed in Figure 3.11, the SHAP model comprehensively explains the areas where Tuberculosis disease may exist in both negative and positive directions, providing more detailed information about whether the individual has Tuberculosis. In Figure 3.12, the LIME model outlines the regions where Tuberculosis disease could be present. Upon examining these results, it is observed that, compared to LIME, SHAP provides better results in explaining Tuberculosis disease.

An example of artificial intelligence explainable to the FP example of the confusion matrix:

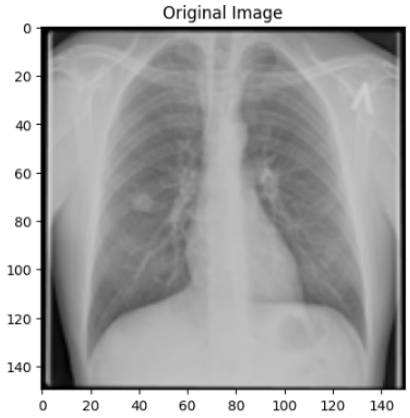

Figure 3.13: Original image

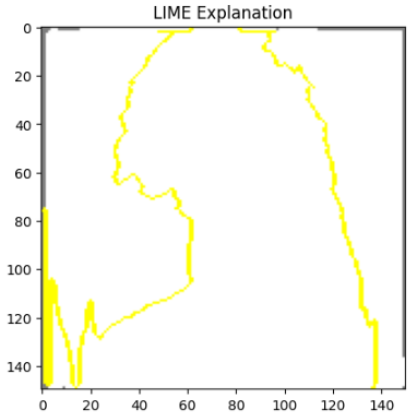

Figure 3.14: LIME output

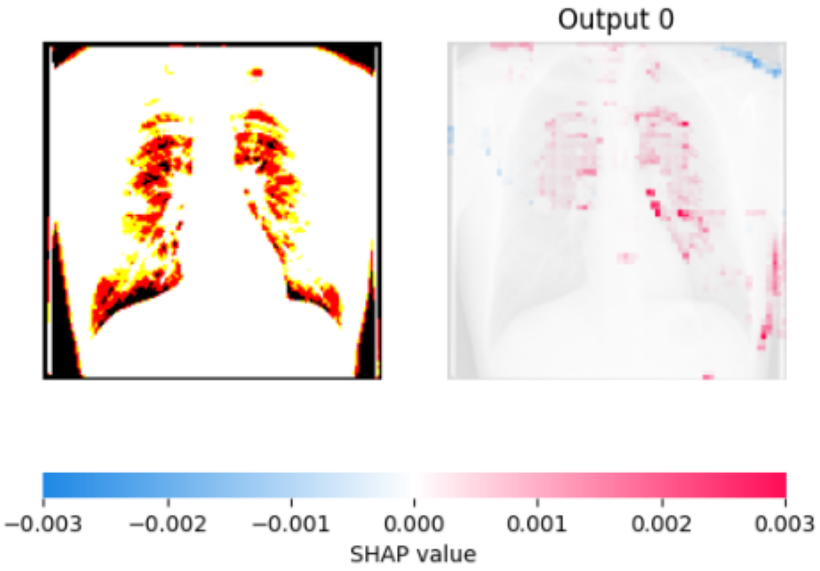

Figure 3.15: SHAP output

The confusion matrix derived from the results of our CNN model applied to the Tuberculosis (TB) Chest X-ray Database specifically showcases a randomly selected example of instances with Tuberculosis disease (FP) in Figure 3.13. The results obtained by applying explainable artificial intelligence models, SHAP and LIME, to this example are presented in Figures 3.14 and 3.15, respectively. As seen in Figure 3.15, the applied SHAP model elaborately explains the areas where Tuberculosis disease may be present in the positive direction, providing more detailed information about the likelihood of the individual having Tuberculosis. In Figure 3.14, the applied LIME model outlines the boundaries where Tuberculosis disease could exist. Upon examining these results, it is observed that SHAP performs better in explaining Tuberculosis disease compared to LIME.

An example of artificial intelligence explainable to the FN example of the confusion matrix:

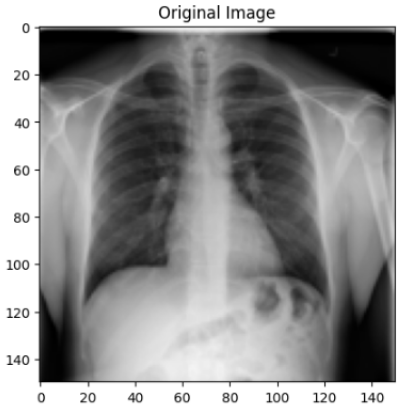

Figure 3.16: Original image

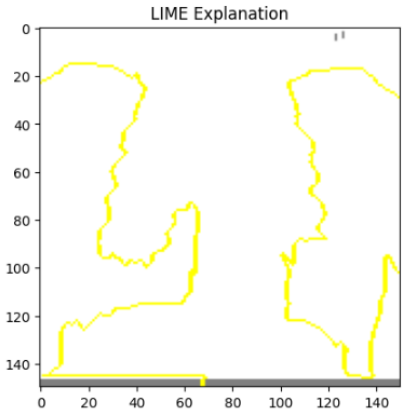

Figure 3.17: LIME output

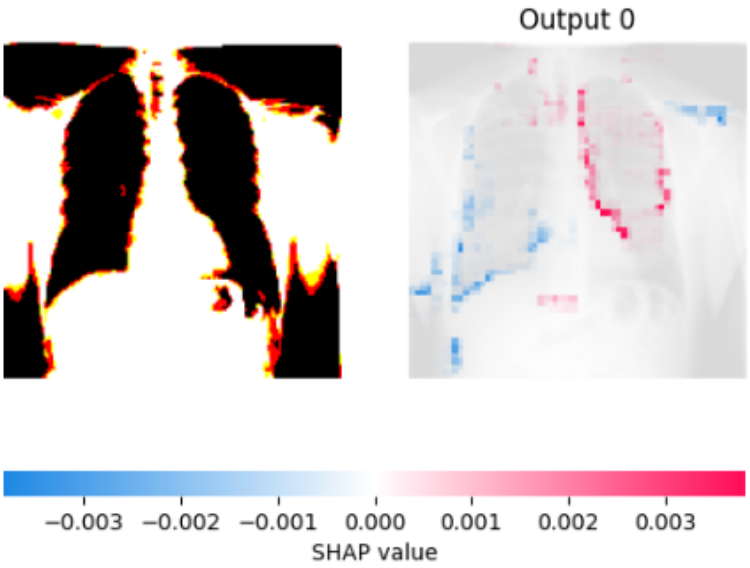

Figure 3.18: SHAP output

An image representing a case of Tuberculosis (TB) with false predictions of the absence of the disease, randomly selected from FN instances in the confusion matrix of our applied CNN model on the Tuberculosis Chest X-ray Database, is presented in Figure 3.16. Results obtained by applying explainable artificial intelligence models, SHAP and LIME, to this example are shown in Figures 3.17 and 3.18, respectively. As seen in Figure 3.18, the applied SHAP model elaborately explains the areas where Tuberculosis disease may be present in both negative and positive directions, providing more detailed information about the individual's likelihood of not having Tuberculosis. In Figure 3.17, the applied LIME model outlines the boundaries where Tuberculosis disease could exist, as shown in Figure 3.16. Upon examining these results, it is observed that SHAP performs better in explaining the absence of Tuberculosis compared to LIME.

An example of artificial intelligence explainable to the TN example of the confusion matrix:

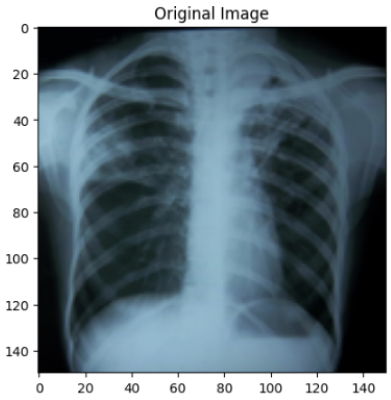

Figure 3.19: Original image

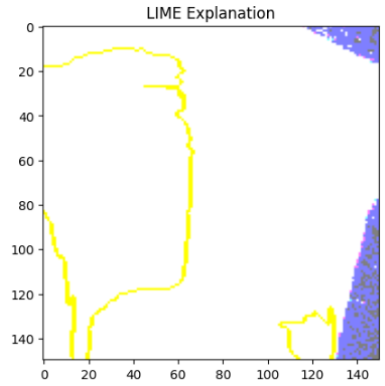

Figure 3.20: LIME output

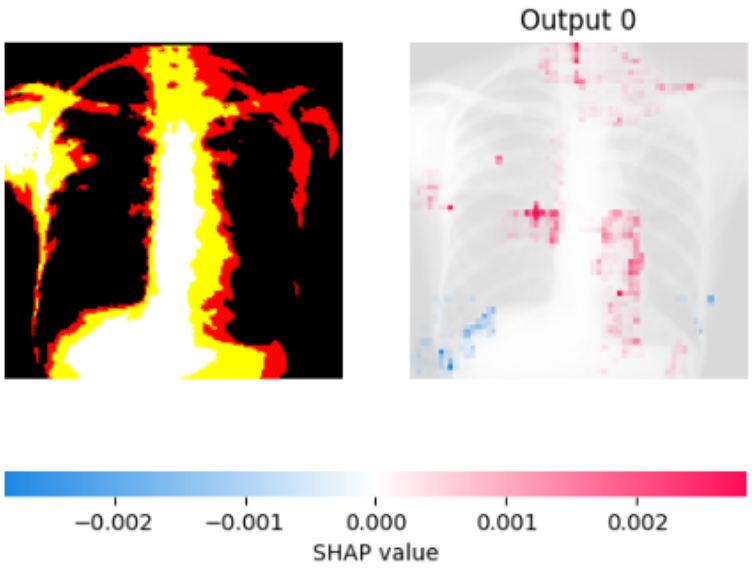

Figure 3.21: SHAP output

An image illustrating a case randomly selected from the TN instances of the confusion matrix of our CNN model applied to the Tuberculosis (TB) Chest X-ray Database, where the disease is not present but a wrong prediction of the individual being diseased has been made, is provided in Figure 3.19. Results obtained by applying explainable artificial intelligence models, SHAP and LIME, to this example are presented in Figures 3.20 and 3.21, respectively. As seen in Figure 3.21, the applied SHAP model elaborately explains the areas where Tuberculosis disease may be present in both negative and positive directions, providing more detailed information about the absence of Tuberculosis in the individual. In Figure 3.20, the applied LIME model outlines the boundaries where Tuberculosis disease could exist, as shown in Figure 3.19. Upon examining these results, it is observed that SHAP performs better in explaining the absence of Tuberculosis compared to LIME.

4. Conclusions

In this study, artificial intelligence (AI) applications in the diagnosis of tuberculosis (TB) were examined in depth. Specifically, the focus was on developing a Convolutional Neural Network (CNN) model for the classification of TB chest X-ray images. Explainable artificial intelligence (XAI) techniques such as SHAP (SHapley Additive exPlanations) and LIME (Local Interpretable Model-agnostic Explanations) were integrated to make the decision-making processes of this model more understandable.

Such mathematical model-based techniques contribute to making models used in medical imaging applications more transparent, understandable, and trustworthy.

The research addressed a significant issue faced by AI applications in the healthcare domain: lack of transparency and reliability. Through the use of XAI techniques, it was demonstrated that the decisions of AI models can be made more understandable. This increases trust in AI-supported diagnostic systems in clinical settings and enables healthcare professionals to make more informed decisions.

In particular, through the comparison of XAI techniques such as SHAP and LIME, SHAP was found to be more effective in TB diagnosis. SHAP provided more reliable and detailed information on the presence or absence of TB disease by offering detailed explanations in the

classification of X-ray images.

Future research should focus on further development and integration of XAI techniques for medical imaging applications. This can enhance the reliability of AI models and enable their more effective use in clinical applications. Additionally, conducting in-depth analyses with larger datasets and using different XAI techniques is critical for improving the performance of AI models.

The results of this study demonstrate that enhancing the reliability and effectiveness of AI-based diagnostic methods in medical imaging can positively contribute to patient treatment and recovery processes. Therefore, future research should focus on broader and more effective use of XAI techniques and making AI models more reliable.

Article Information

Author's contributions: or The article has a single author. The author has read and approved the final manuscript.

Conflict of Interest Disclosure: The author declare that he has no known competing financial interests or personal relationships that could have appeared to influence the work reported in this paper.

Supporting/Supporting Organizations: The author gratefully acknowledge the financial support of Sakarya University of Applied Sciences AI And Data Science Research And Application Center.

Ethical Approval and Participant Consent: This research adheres to ethical principles and guidelines in conducting the comparative analysis of Explainable Artificial Intelligence (XAI) techniques, specifically SHAP (SHapley Additive exPlanations) and LIME , on tuberculosis x-ray dataset.

Plagiarism Statement: This article was scanned by the plagiarism program. No plagiarism detected.

Availability of data and materials: tawsifurrahman/tuberculosis-tb-chest-xray-dataset".

References

[1] C. Liu, Y. Cao, M. Alcantara, B. Liu, M. Brunette, J. Peinado, *W. Curioso, TX-CNN: Detecting tuberculosis in chest x-ray images using convolutional neural network*, IEEE Int. Conf. Image Process. (ICIP), 2017.
[2] U.K. Lopes, J.F. Valiati, *Pre-trained convolutional neural networks as seature extractors for tuberculosis detection*, Comput. Biol. Med., 2017.
[3] S. Mahamood, Explainable artificial intelligence and its potential within industry, in Proc. 1st Workshop Interactive Nat. Lang. Technol. Explainable Artif. Intell. (NL4XAI), J.M. Alonso, A. Catala (Eds.), Association for Computational Linguistics, 2019.
[4] R. Guo, K. Passi, C.K. Jain, *Tuberculosis diagnostics and localization in chest x-rays via deep learning models*, Front. Artif. Intell., **3** (2020), 583427.
[5] B. Oltu, S. Güney, B. Dengiz, M. Ağıldere, *Automated tuberculosis detection using pre-trained CNN and SVM*, 44th Int. Conf. Telecommun. Signal Process. (TSP), 2021.
[6] S. Stanišić, M. Perišić, G. Jovanović, D. Maletić, D. Vudragović, A. Vranić, A. Stojić, *What Information on Volatile Organic Compounds Can Be Obtained from the Data of a Single Measurement Site Through the Use of Artificial Intelligence?*, Artificial Intelligence: Theory Appl., E. Pap (Ed.), Springer International Publishing, 2021.
[7] D. Chakraborty, A. Alam, S. Chaudhuri, H. Başağaoğlu, T. Sulbaran, S. Langar, *Scenario-based prediction of climate change impacts on building cooling energy consumption with explainable artificial intelligence*, Appl. Energy, **291** (2021), 116807.
[8] B.H.M. van der Velden, H.J. Kuijf, K.G.A. Gilhuijs, M.A. Viergever, *Explainable artificial intelligence (XAI) in deep learning-based medical image analysis*, Med. Image Anal., **79** (2022), 102470.
[9] A.D. Orjuela-Cañón, A.L. Jutinico, C. Awad, E. Vergara, A. Palencia, *Machine learning in the loop for tuberculosis diagnosis support*, Front. Public Health, **10** (2022, 876949.
[10] H.H. Rashidi, I.H. Khan, L.T. Dang, S. Albahra, U. Ratan, N. Chadderwala, W. To, P. Srinivas, J. Wajda, N.K. Tran, *Prediction of tuberculosis using an automated machine learning platform for models trained on synthetic data*, J. Pathol. Inform., **13** (2022), 100172.
[11] A. Wong, J.R.H. Lee, H. Rahmat-Khah, A. Sabri, A. Alaref, H. Liu, *TB-Net: A tailored, self-attention deep convolutional neural network design for detection of tuberculosis cases from chest x-ray images*, Front. Artif. Intell., **5** (2022), 827299.
[12] T. Yiğit, N. Şengöz, Ö. Özmen, J. Hemanth, A.H. Işık, *Diagnosis of paratuberculosis in histopathological images based on explainable artificial intelligence and deep learning*, Traitement du Signal, **39**(3), 2022, 863-869.
[13] J. Purohit, I. Shivhare, V. Jogani, S. Attari, S. Surtkar, *Adversarial Attacks and Defences for Skin Cancer Classification*, *2023 Int. Conf. Adv. Technol. (ICONAT)*, IEEE, Jan. 2023.
[14] A.R. Bhatt, R. Vaghashiya, M. Kulkarni, P. Kamaraj, *Explainable artificial intelligence in retinal imaging for the detection of systemic diseases*, 2022.
[15] S. Hansun, A. Argha, S.-T. Liaw, B.G. Celler, G.B. Marks, *Machine and deep learning for tuberculosis detection on chest x-rays: systematic literature review*, J. Med. Internet Res., **23** (2023), e43154.
[16] H. Hajiyan, M. Ebrahimi, *Multi-scale local explanation approach for image analysis using model-agnostic explainable artificial intelligence (XAI)*, in Med. Imaging 2023: Digital Comput. Pathol., J.E. Tomaszewski, A.D. Ward (Eds.), SPIE, 2023.
[17] N.E. Jaimes, C. Zeng, R. Simha, *Using biologically hierarchical modular architecture for explainable, tunable, generalizable, spatial AI*, in Disruptive Technol. Inf. Sci. VII, M. Blowers, J. Holt, B.T. Wysocki (Eds.), 2023.
[18] F. Mahmud, M.M. Mahfiz, M.Z.I. Kabir, Y. Abdullah, An Interpretable deep learning approach for skin cancer categorization, 2023.
[19] NIAID TB portal program dataset [Online]. Available: https://tbportals.niaid.nih.gov/download-data.
[20] M.M. Hasan, M.M. Hossain, M.M. Rahman, A.K. Azad, S.A. Alyami, M.A. Moni, *FP-CNN: Fuzzy pooling-based convolutional neural network for lung ultrasound image classification with explainable AI*, Comput. Biol. Med., **165** (2023), 107407.
[21] E. Shoemaker, H. Malik, H. Narman, J. Chaudri, *Explaining the unseen: Leveraging XAI to enhance the trustworthiness of black-box models in performance testing*, Proc. Comput. Sci., **224** (2023), 83-90.
[22] R. Younisse, A. Ahmad, Q. Abu Al-Haija, *Explaining intrusion detection-based convolutional neural networks using Shapley additive explanations (SHAP)*, Big Data Cogn. Comput., **6**(4) (2022), 126.